Microwave Propulsion Ionizer

Donald G. Johansen - EMF Kinetics
13450 Pescadero Creek Road, La Honda, California, U.S.A.
johansen.d@att.net

Abstract

High power microwave sources are now available and usable, with modification, for beamed energy propulsion experiments in space. As output windows and vacuum seals are not needed space is a natural environment for high power vacuum tubes. Application to space therefore improves reliability and performance but complicates testing and qualification. Low power microwave devices (TWT, etc) have already been through the adapt-to-space design cycle and this history is a useful pathway for high power devices such as gyrotrons. Microwave propulsion devices require ionized component from 10 to 100 ppm in order to transfer beam energy to propellant. Two types of ionizers are considered in this paper. First, the ***arc jet*** device is space-qualified as propulsion device but consumes high power. Second, the microwave discharge ionizer creates in-chamber ions by injection of seed gas into one or more focal regions near the dome part of the chamber.

1. INTRODUCTION

Beamed energy propulsion (BEP) was originally proposed for earth-based launch using lasers [1] or microwave [2]. High-power microwave gyrotrons now produce continuous 1 MW power near 1 millimeter wavelength. Beam intensity is high at high chamber pressures needed for earth-based launch and gas breakdown occurs. Microwave discharge phenomena are avoided at low pressure as beam intensity is reduced. Low pressure implies high exit diameter and this increases beam range which is beneficial. These factors lead to consideration of space or lunar-based beamed energy propulsion.

Lunar-based BEP was proposed to provide transport of lunar cargo and refuel oxidizer to command module for return-to-earth Apollo-type mission [3]. Using lunar oxygen propellant (LUNOX) the propellant mass to achieve low lunar orbit is approximately equal to payload mass. The Lunar Shuttle Vehicle (LSV) reduces earth-launch mass by a factor of three. Although chemical propulsion would provide the same reduction, fuel is not available over the full lunar surface. Hence, BEP enables exploration over 100% of lunar surface while chemical propulsion using LH2 and LO2 derived from lunar water is restricted to lunar pole regions.

2. VEHICLE CONCEPT

Figure 1a shows thruster profile and Figure 1b shows vehicle configuration of Lunar Shuttle Vehicle which is designed to transport 100 kg payload from the lunar surface to low lunar orbit (LLO). The reflecting nozzle is built in two sections. A conical section is attached to the throat and ends at a curved section. Regenerative cooling occurs with propellant entering the cone end pathway and continues into the chamber pathway toward the dome where injection into the chamber occurs. Heat is removed from the curved section by radiation cooling.

For each nozzle, the beamed energy is approximated by parallel rays crossing the nozzle exit plane. Figure 1a trace lines depict paths of circular sections after reflection from the inner nozzle.

The nozzle area ratio is 20:1 and projected area provides 5% of beamed energy to central region via throat. Area projected by conical and curved sections captures 20% and 75% of beamed energy, respectively. Beamed power per nozzle is above 1 MW. Assuming 50% of central region power reaches the dome, the available power for ionization is above 25 KW.

Ionizer output can be expressed as electric current in Amperes and approximately 100 A are needed per 1 MW thruster. For 4 Volts ionization energy, the theoretical power is 400 Watts which is well under available 25 KW power.

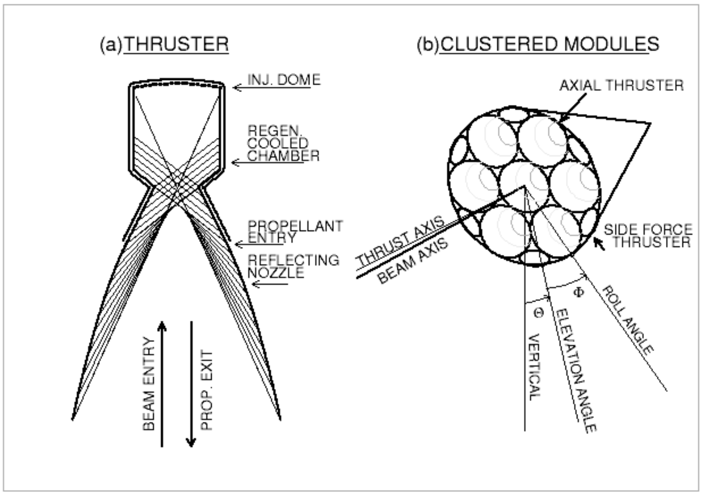

Figure 1. Beamed Energy Thruster and Platform Concept.

3. ARCJET DOME IONIZER

Details of thruster dome design are shown in Figure 2. Figure 2a shows ionizer based on arc jet thruster, a space proven device used for orbit maintenance. Figure 2b shows ionizer based on microwave discharge phenomena.

Beam absorption requires 10-100 ppm ion density at temperatures from 800 to 4000K. Near 1 atm pressure, thermal ionization provides suitable ion fraction above 3000K. However, at lower temperatures, the ion fraction decreases and suitable absorption cannot be obtained. This problem is solved by injecting high temperature Argon gas which is mixed with Potassium seed concentrated near 1%. This requires injection temperatures exceeding 4000K. As this is above melting temperature of all metals, conventional heat exchangers cannot be used. Shown in Figure 2a, ions are thermally created within injected gas by DC arc which is centered in arc jet bore [4].

Seed/host gas mixing is shown in Figure 3. Seed elements, Cesium or Potassium, have melting points of 302K and 337K respectively. Full evaporation to gas phase at one atmosphere occurs at 952K and 1047K, respectively. As shown in Figure 3, a 10% unionized gas mixture is created in the mixing chamber at 800K according to vapor pressure relationship of metallic gas [5]. (See Figure 3) This mixture enters arc jet at cathode end and thermal ions are created as the gas is arc-heated. The ionized mixture exits into the chamber, passing the anode at 5000K temperature.

Injected seed concentration is somewhat higher than thrust chamber concentration levels. Ions are diffused into the propellant gas before exiting the dome region. Electron energy is above thermal levels due to microwave field and ambipolar diffusion aids mixing of ions with propellant.

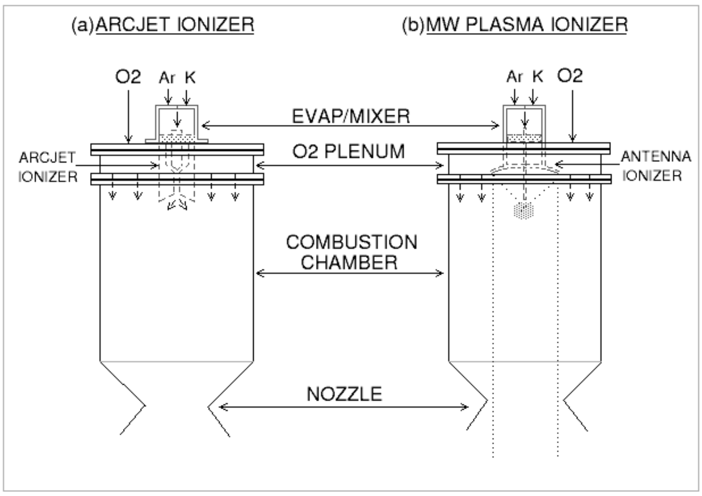

Figure 2. Ionizer Concept using Arcjet Device and Microwave Discharge.

The arcjet obtains heating power from DC bus which requires several kilowatts per thruster. Also, several ionizers are needed for each thruster as ions must be distributed away from centerline to obtain attenuation near chamber wall. This complexity leads to consideration of microwave discharge ionizer. This method uses the same mixer device to regulate seed flow but uses microwave field energy directly to create ions.

4. MICROWAVE PLASMA DOME IONIZER

The microwave discharge ionization process is shown in Figure 2b [4]. High concentration Ar:K mixture at 800K enters the discharge region as shown. Flow carries the seed gas through the center core which is rapidly heated well above ionization temperature. Electrons with ion partners diffuse outside discharge region to fill dome region.

Details of microwave discharge are well known [5]. The high intensity electric field near the focal point causes avalanche production of plasma. This plasma strongly absorbs the beam and expands outward toward the beam. A stationary radius occurs where ion density is lowered such that plasma frequency is below beam frequency.

The progress of electron/ion pairs beyond the plasma radius is due to ambipolar diffusion. Electrons maintain high energy due to the residual beam near the dome. Ambipolar diffusion drives electron/ion pairs to all dome regions so beam absorption is achieved.

Performance requirements for the plasma ionizer are shown in Table 1. Values are given for chamber pressures of 0.5 and 2.0 atmospheres. From Figure 3, pressure and temperature of seed/host mix chamber are above chamber pressure and temperature [6]. At 0.5 atm near saturation, the desired 10% seed fraction is obtained at 800K. At 2 atm, 10% saturation occurs at 900K. Propellant flows of 0.33 and 1.32 kg/sec with ion fractions of 100 and 12.5 ppm occur at pressures of 0.5 and 2.0 atm, respectively for the 12 cm nozzle.

Table 1 - Calculated Ion Seed Flow for Microwave Discharge Ionizer.

host:seed	Pres0	Temp0	Propellant Mass Flow	Ion Fraction	Ion Seed Mass Flow	Seed+Host Mass Flow	Ion Current
Ar:K 9:1	0.5 atm	800 K	0.33 kg/sec	100 ppm	0.0415 g/sec	0.415 g/sec	100 Amp.
Ar:K 9:1	2.0 atm	800 K	1.32 kg/sec	12.5 ppm	0.0208 g/sec	0.208 g/sec	50 Amp.

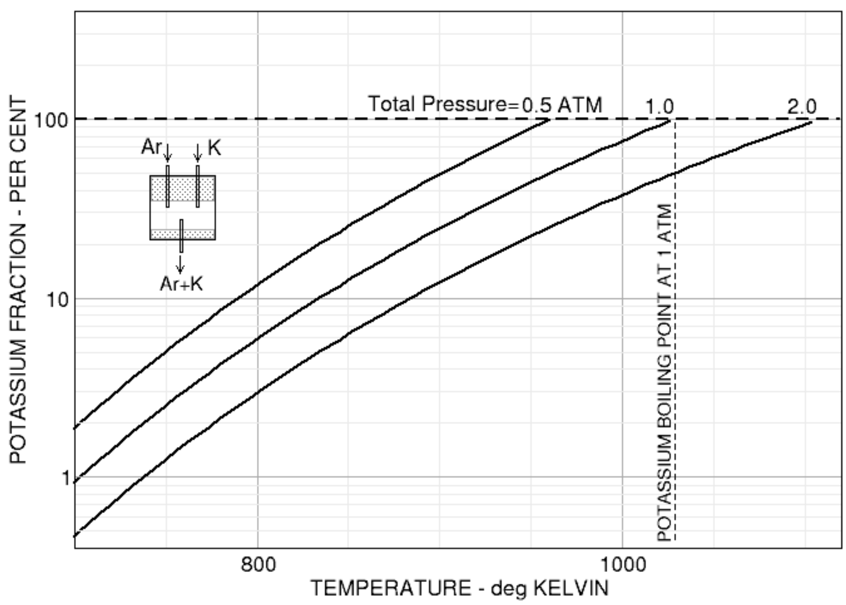

Figure 3. Seed Gas Mixture Fraction vs. Temperature and Pressure

Ionization is produced by energetic electrons within the plasma radius. To ionize Cesium or Potassium, the energy must exceed 4 electron volts. Plasma diameters for three dome focus strategies are shown in Figure 4. These curves are based on Argon host gas and available beam power at dome center. The top curve shows the concave mirror reflecting to centerline. This approach is illustrated in Figure 2b. This method produces an acceptable plasma diameter (greater than 20 mm.) to well above 500 GHz. The spot size vs. frequency is not a diffraction effect but is due to inverse relation of electron energy with frequency squared. This varies spot size inversely with frequency as higher intensity occurs near focal point.

The bottom curve shows plasma diameter of torus ring produced by symmetric mirror reflecting away from centerline. Due to continuous distribution over circumference, the plasma diameter is less than 20 mm at 160 GHz and likely to be ineffective above 200 GHz.

A better result is obtained when the central mirror divides the center beam to create 6 focal points. This plasma diameter is shown by the center curve in Figure 4. Spot size is above 30 mm at 200 GHz, usable at 300 GHz and marginal above 500 GHz.

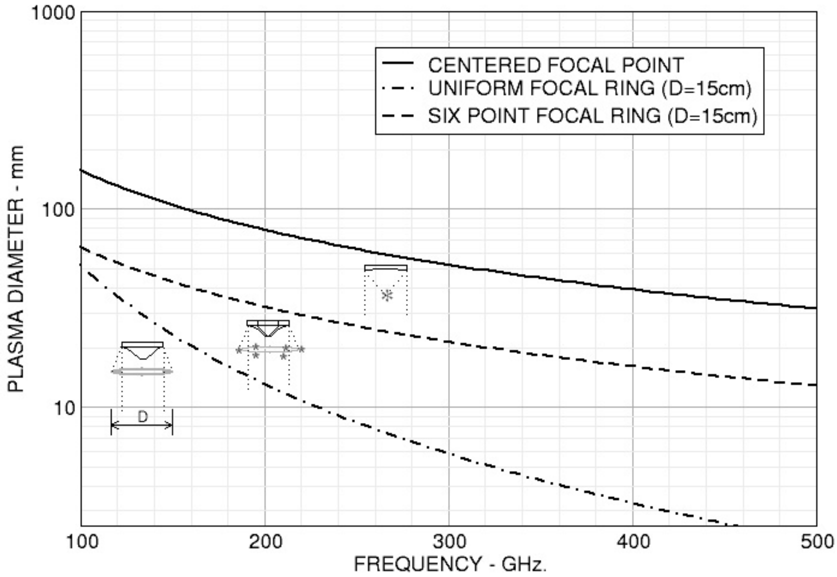

Figure 4. Plasma Spot Diameter Produced by 25 KW Central Beam.

5. ION/PROPELLANT MIXING

A multiple mirror plasma ionizer is shown Figure 5. This design would be appropriate for a flight size thruster with nozzle diameter of 12 cm. Injection away from the center is also needed to avoid blocking the central beam which is energy source of ionization. Seed/host mixing in a heated chamber precedes injection into the combustion chamber.

Diffusion of ions into propellant gas is calculated as follows: Free electron energy (expressed in volts) is given by:

$$U_e = (e/m)E^2 / (\omega^2 \delta) \tag{1}$$

where e/m is electron charge to mass ratio, E is electric field strength, ω is beam radian frequency and δ is electron energy fraction lost per collision. This equation applies when electron kinetic energy is above thermal energy. The diffusion coefficient is calculated as:

$$D = \sqrt{U_e (e/m)/6} / N\sigma \tag{2}$$

where N is gas particle density and σ is electron collision cross section. Solution of the diffusion equation applies, with diffusion wavefront growing as sqrt(2Dt). For low electric field, electrons are at thermal temperature and diffusion coefficient for ambipolar diffusion is used.

$$D = \sqrt{kT_e / 4m} / N\sigma \tag{3}$$

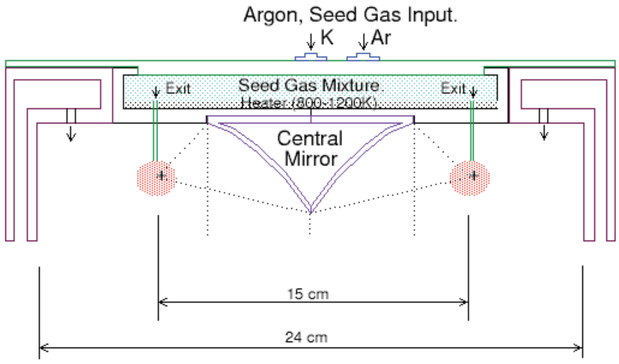

Figure 5. Microwave Plasma Ionizer with Seed/Host Mixer.

6. ION EFFECTIVENESS

Energetic electrons emerge from the seed/host injected gas and, due to kinetic energy, diffuse into the propellant. Removed from the host gas, the electrons produce an electric field which draws partner ions from the host gas. This process is called ambipolar diffusion. Due to low electron mass and high kinetic velocity, rapid ion distribution results from this process.

Ion recombination is a possible ion loss mechanism which could reduce effectiveness of the ionizer. Experience indicates that recombination does occur at chamber wall but less so within the gas [7]. Three-body collisions are needed for recombination, but within the gas this occurs rarely. Two-body collisions (electron + positive ion) occur frequently. However, before colliding with an ion, the electron has energy due to approach velocity which must be combined with potential energy. The total energy is greater than ionization energy and, unless a third body is present to carry off excess energy, the deionization does not occur and the interaction counts as an elastic collision.

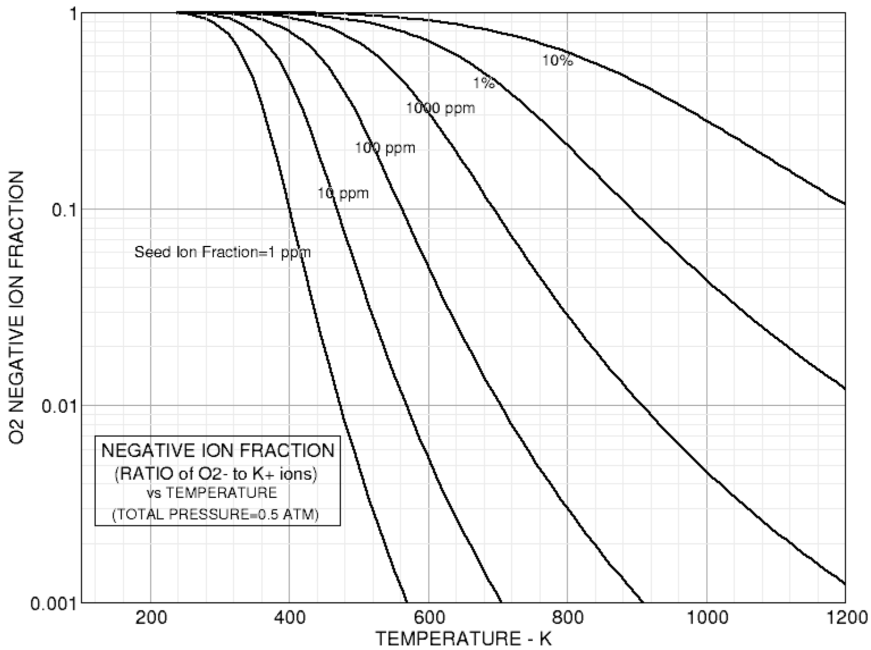

Figure 6. O2 Negative Ions as Fraction of Total Seed Ions.

Combination of potassium with molecular oxygen must also be considered as loss mechanism of ions. As K+ ion and O2 are strongly electronegative (high electron affinity) they cannot combine readily to produce KO2+ ion. There remains possibility of electron attachment producing O2- ion and subsequent combination with K+ to produce neutral KO2. Figure 6 shows equilibrium number of negative ions as a fraction of total ions [8]. For gas temperatures increasing above 800K, negative ions decrease rapidly for total ion fractions below 1%. For example, at 800K with total ion fraction of 1%, the possibility of ion combination occurs once per 500 collisions. (Ion approach geometry reduces likely combinations per collision to well below 1/500.) It is evident that few ions are lost at temperatures above 800K and total ion fractions below 1%.

7. SIMULATION RESULTS

Flow simulation for 12 cm throat diameter nozzle operating at chamber pressure of 0.5 atm is shown in Figure 7. Thrust level is 926 Newtons. Oxygen propellant with ideal properties is assumed. Beam power is 1.2 MW and frequency is 300 GHz. Gas heating is due to collected beam entering the nozzle throat at station zero. Ions are injected near the dome and chamber wall in a circular ring with diameter of 75 mm. The combined effects of ion transport by convection and diffusion are shown in Figure 7 (top graph). Beam attenuation due to ion distribution is shown in middle graph and temperature contours are shown in the lower graph. The beam attenuation coefficient, K (expressed in inverse meters), is calculated as:

$$K / nN = \sigma\sqrt{2/\delta} \cdot (e/m)^2 eEZ / \omega^3 \tag{4}$$

E is electric field intensity and Z=2p60 is impedance of space.

The wavelength is 1 mm and the throat diameter is 120 wavelengths. Beam attenuation in the chamber is calculated using ray trace model for cylindrical coordinates. Diffraction effects would occur as chamber length approaches 120 diameters. The chamber length is 3 throat diameters so ray tracing is valid for this simulation.

For a circular nozzle, the reflected beam is concentrated near the centerline and this explains the distribution of high temperature along the centerline. This results in low gas density in the central core which allows 50% of the central beam to reach the dome mirror. Thus, for large nozzles excess ionization power is available. Low gas density and beam concentration also cause fast diffusion. From the top graph it is seen that ions diffuse mainly to the center but also forward and outward to reach the chamber wall where they are recombined. The central ions also diffuse toward the wall in the downstream region but a portion exits through the throat.

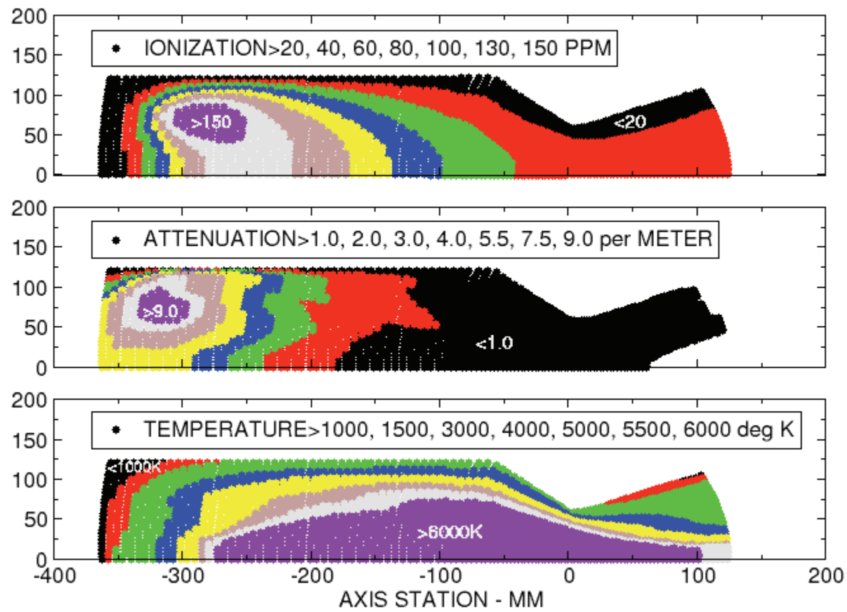

Figure 7. Flow Simulation Contours for Flight Thruster.

8. CONCLUSIONS

The Arcjet ionizer requires substantial DC power (above 10 KW per thruster) and is subject to anode erosion which limits lifetime. Although the Arcjet thruster is space qualified, need for DC power supply adds mass and complexity which degrades performance and reliability.

The Microwave Plasma Ionizer uses microwave energy near the dome region to create ions. Microwave discharge occurs in the gas away from walls so that erosion does not occur. Added equipment includes in-chamber mirror and outside seed/host mixer operating at 800 deg K near 1 atm pressure. Also, seed/host storage and flow regulation impose additional system needs.

Simulation shows that the central core of the nozzle allows the beam to pass to dome region with low attenuation. This is due to concentration of reflected beam and subsequent high temperature and low density near centerline. This effect allows sufficient power for microwave discharge ionization near dome region. Ambipolar diffusion is a major factor causing distribution of ions leading to efficient beam absorption in the chamber.

REFERENCES

[1] A.Kantrowitz, Propulsion to Orbit by Ground-Based Lasers, *Astronautics &Aeronautics*, 10, No.5, (1972) pp. 74-76.

[2] J.Benford, R. Dickinson, Space Propulsion and Power Beaming using Millimeter Systems, *Intense Microwave Pulses III*, H. Brandt, Ed., SPIE 2557, 179 (1995). Also published in Space Energy and Transportation. 1, 211 (1996).

[3] D.G.Johansen, Lunar Oxygen as Monopropellant, (ISBP5), AIP Conf. Proceedings 997 p.507-519 (2008).

[4] D.G.Johansen, Space Experiments to Advance Beamed Energy Propulsion, (ISBP6), AIP Conf. Proc. (2009 in print).

[5] V.G.Brovkin, Y.F.Kolesnichenko. MW Energy Addition in Application to Propulsion. (ISBP1), AIP Conf.Proceedings 664 p.268-279 (2002).

[6] K.J.Bowles. Vapor Pressure of Potassium to 2170 K. NASA TND-4535 Lewis Research Center, Cleveland Ohio, May 1968.

[7] J.D.Cobine, Gaseous Conductors. pp 78-107. Dover Publications, Inc. New York.

[8] M.Sulka,et.al,Electron Affinity of O2 Molecules. Int. J. of Quantum Chemistry, Vol.108, Issue 12, pp.2159-2171.